MECHANIKA TEORETYCZNA
I STOSOWANA
Journal of Theoretical
and Applied Mechanics
1, 30, 1992

# DEVELOPMENT OF THE OBLIQUE INCIDENCE METHOD BASED ON THE LIGHT SCATTERING PHENOMENON

MAREK SIKOŃ

*Cracow University of Technology*

General relationships for photoelastic investigations in the form of a system of equations containing components of a stress tensor and parameters of a light field running through the tested medium have been formulated in this paper.
Investigations are carried out on the basis of the oblique incidence method together with the observation of scattered light.
A description of a plane electromagnetic wave in anisotropic medium is presented in appendix 1. This analysis has been adopted for photoelastic needs and combined with the concept of stresses optically active (secondary principal stresses).
Appendix 2 contains the experimental part of the work. Results of the experimental and the analysis of the error prove the assumed relationships correctness and the generality of the method.
This paper is the starting point for the analysis of the compound states of stress.

## 1. Introduction

Components of the stress tensor

$$\begin{bmatrix} \sigma_x & \tau_{xy} & \tau_{xz} \\ \tau_{yx} & \sigma_y & \tau_{yz} \\ \tau_{zx} & \tau_{zy} & \sigma_z \end{bmatrix} \tag{1.1}$$

in photoelastic medium are determined on the basis of the birefringence phenomenon. Tensor (1.1) is symmetrical and thus the number of unknowns is reduced to six.

The majority of works on photoelasticity present solutions to particular problems of strength of materials.

The aim of this paper is to show the system of six independent equations containing complete components of the stress tensor (1.1) and coefficients of a light field running through the tested medium. Such investigations can serve as a starting point for the experimental solution of complex cases of strength of materials. The oblique incidence method [1] and observation of scattered light [2] have been combined in this work.

## 2. Optical and mechanical properties of photoelastic medium

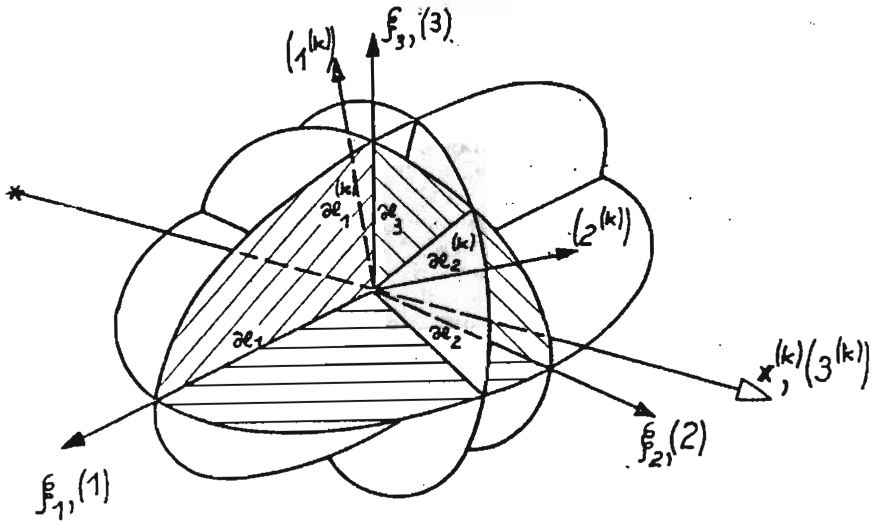

Fig. 1. Optical ellipsoid. $(\xi_1, \xi_2, \xi_3)$ – coordinate system of optical ellipsoid; (1),(2),(3) – principal axes of the tensor $\kappa_{ij}$; $1^{(k)}, 2^{(k)}, 3^{(k)}$ – quasi–principal directions; $\kappa_1^{(k)}, \kappa_2^{(k)}$ – quasi–principal coefficients of dielectric permittivity; $x^{(k)}$ – direction of the course of light

Properties of a photoelastic medium can be described with the aid of a quadratic surface, the so–called optical indicatrix (Fig.1). This surface referrs to the coordinate system $(\xi_1, \xi_2, \xi_3)$ connected with the permittivity dielectric tensor $\kappa_{ij}$ principal axes (1.1), (2.1), (2.2) in the form of equation

$$\frac{\xi_1^2}{\kappa_1^2} + \frac{\xi_2^2}{\kappa_2^2} + \frac{\xi_3^2}{\kappa_3^2} = 1 \tag{2.1}$$

where: $\kappa_1$, $\kappa_2$, $\kappa_3$ – permittivity dielectric coefficients in (1.1), (2.1) and (2.2) directions respectively.

Generally an indicatrix is an ellipsoid with its axes directed along (1.1), (2.1), (2.2) and lengths of semi–axes equal to $\kappa_1$, $\kappa_2$, $\kappa_3$ (Fig.1).

In the tested medium two lineary polarized waves propagate at different velocities $v'$, $v''$ in an optional direction $x^{(k)}$ (index $k$ denotes the successive direction of the course of light). These waves vibrate on the plane perpendicular to $x^{(k)}$ in quasiprincipal directions $(1^{(k)})$, $(2^{(k)})$ (appendix 1).

To determine directions $(1^{(k)})$, $(2^{(k)})$ we have to out the indicatrix with the plane running through the origin of the coordinate system $(\xi_1, \xi_2, \xi_3)$ and normal to $x^{(k)}$. As a result we get an ellipse semi–axes of which are directed in $(1^{(k)})$, $(2^{(k)})$, and with the lengths equal to quasi–principal permittivity dielectric coefficients (Fig.1). (Direction $(3^{(k)}$ overlaps $x^{(k)}$, permittivity coefficient along $(3^{(k)})$ is denoted $\kappa_3^{(k)}$).

Photoelastic medium satisfies assumptions of material continuum and its mechanical properties are described by the stress tensor.

Tensor components $\sigma_{ij}$ and $\kappa_{ij}$ in linear range are bounded by the law which, for quasi–principal directions, can be presented in the followng way

$$\begin{aligned}
\kappa_1^{(k)} &= \kappa_0 + C_1\sigma_1^{(k)} + C_2(\sigma_2^{(k)} + \sigma_3^{(k)}) \\
\kappa_2^{(k)} &= \kappa_0 + C_1\sigma_2^{(k)} + C_2(\sigma_1^{(k)} + \sigma_3^{(k)}) \\
\kappa_3^{(k)} &= \kappa_0 + C_1\sigma_3^{(k)} + C_2(\sigma_1^{(k)} + \sigma_2^{(k)})
\end{aligned} \tag{2.2}$$

where

- $\kappa_0$ – permittivity dielectric coefficient in stressed free medium,
- $C_1, C_2$ – optical cconstants,
- $\sigma_1^{(k)}, \sigma_2^{(k)}, \sigma_3^{(k)}$ – stress components in directions $(1^{(k)})$, $(2^{(k)})$, $(3^{(k)})$, respectively.

Stresses $\sigma_1^{(k)}$, $\sigma_2^{(k)}$, $\sigma_3^{(k)}$, satysfying the law (2.2) are known in photoelasticity as stresses optically active or as secondary principal stresses.

Electric field waves vibrating in the following directions

$$\begin{aligned}
u_k &= a_k \cos\omega t \\
w_k &= b_k \cos(\omega t + \psi_k)
\end{aligned} \tag{2.3}$$

where

- $\omega$ – frequency of light,
- $a_k, b_k$ – amplitudes of electric field intensity vectors vibrating in directions $(1^{(k)})$, $(2^{(k)})$,
- $t$ – time,
- $\psi_k$ – phase of the $w_k$ wave with respect to $u_k$,

become relatively retarded on the elementary path $\delta x_k$ by the value of $\frac{2\pi}{\lambda}(n_1^{(k)} - n_2^{(k)})\delta x_k$

$$u_k = a_k \cos \omega t$$
$$w_k = b_k \cos\Big[\omega t + \psi_k + \frac{2\pi}{\lambda}(n_1^{(k)} - n_2^{(k)})\delta x_k\Big] \tag{2.4}$$

where

$n_1^{(k)}, n_2^{(k)}$ – refraction coefficients in directions $(1^{(k)})$ and $(2^{(k)})$ respectively,

$\lambda$ – length of the wave light running through the tested medium.

Taking into consideration the rotation of directions $(1^{(k)})$, $(2^{(k)})$ through the value $\delta\lambda_k$, and the modification of both the amplitude and the phase of component waves by the value $\delta a_k$, $\delta b_k$, $\delta\psi_1^k$, $\delta\psi_2^k$ on the path $\delta x_k$ we can write

$$u'_k = (a_k + \delta a_k)\cos(\omega t + \delta\psi_1^k)$$
$$w'_k = (b_k + \delta b_k)\cos(\omega t + \delta\psi_2^k). \tag{2.5}$$

Values $\delta a_k$, $\delta b_k$ and the increase of the phases difference $\delta\psi_k = \delta\psi_2^k - \delta\psi_1^k$ is calculated by combining (2.4) and (2.5). Within the limits of the expressions we look for, we finally get [2]

$$da_k = b_k \cos\psi_k d\alpha_k \tag{2.6}$$

$$db_k = -a_k \cos\psi_k d\alpha_k \tag{2.7}$$

$$d\psi_k = \frac{2\pi}{\lambda}\Big(n_1^{(k)} - n_2^{(k)}\Big)dx_k + \Big(\frac{a_k}{b_k} - \frac{b_k}{a_k}\Big)\sin\psi_k d\alpha_k. \tag{2.8}$$

For electromagnetic waves, frequencies of which are smaller compared to the interatomic ones and the material they go through is a dielectric of a negligibly small electrical conductivity, we can write

$$n_1^{(k)} = \sqrt{\kappa_1^{(k)}}$$
$$n_2^{(k)} = \sqrt{\kappa_2^{(k)}}. \tag{2.9}$$

Combining relations (2.2), (2.8), (2.9) we finally get a formula [2]

$$\frac{\lambda}{2\pi C_\sigma}\Big[\frac{d\psi_k}{dx_k} - \Big(\frac{a_k}{b_k} - \frac{b_k}{a_k}\Big)\sin\psi_k\frac{d\alpha_k}{dx_k}\Big] = (\sigma_1^{(k)} - \sigma_2^{(k)}) \tag{2.10}$$

where

$$C_\sigma = \frac{C_1 - C_2}{2\sqrt{\kappa_0}}$$

binding the state of stress with parameters of a light field running through the photoelastic medium of the point.

A description of examined objeccts is referred to a infinitesimally small, cube element, cut out of the interior of the tested medium, considering this element as the measuring point of the photoelastic medium.

## 3. Scattering of light in photoelastic medium

Photoelastic medium becomes anisotropic when influenced by the loading field. The theory of anisotropic centres is applied to the description of the phenomena of light scattering in photoelastic media.

The photoelastic medium is assumed to be a set of electric dipoles of polarizability $\rho$. A variable electric field falling on this medium induces forced vibrations in it. The electric dipoles become a source of self-radiation frequency of which corresponds with the frequency of falling light (elastic scattering) and for which phase relations between falling and scattered light wave are strictly hold (coherent scattering).

Scattering light coefficient over a volume unit or a mass of photoelastic medium determines the size of the part of energy of a light beam taken by scattered light

$$\eta = \frac{8\pi}{3}(\rho)^2\left(\frac{\omega}{c}\right)^4 \tag{3.1}$$

where
- $\omega$ – frequency of the falling and scaterred light,
- $c$ – speed of light in a vacuum.

For the electron elastically bounded we can write

$$\rho = \frac{e^2}{m_e}(\omega_0^2 - \omega^2 + 2i\gamma\omega) \tag{3.2}$$

where
- $e, m_e$ – electron mass and charge,
- $\omega_0$ – electron natural frequency,
- $\gamma$ – damping decrement,
- i – imaginary unit.

For $\omega$ different much from $\omega_0$, dependency of $\rho$ on $\omega$ can be neglected and the relation

$$\eta \sim \omega^4 \sim \frac{1}{\lambda^4} \tag{3.3}$$

is defined by the Rayleigh's law.

Scattered light intensity $J$ at $\varphi$ angle with respect to the falling beam is described by the Rayleigh's formula

$$J(\varphi) = J_0\Omega_0\Big(\frac{\eta}{4\pi}\Big)\frac{3}{4}(1+\cos^2\varphi) \tag{3.4}$$

where

$J_0$ – intensity of the falling light beam,

$\Omega_0$ – angle of divergence of the falling light beam,

$\varphi$ – scattering angle.

Degree of polarization of the light scattered by a dipole is calculated according to the following formula

$$P(\varphi) = \frac{\sin^2\varphi}{1+\cos^2\varphi}. \tag{3.5}$$

The analysis of the scattered light on the plane perpendicular to the direction $x^{(k)}$ of the light beam (scattering plane), gives the most favourable conditions of observation of polarizing–phasic effects of the tested photoelastic medium.

## 4. Oblique incidence method for determining coefficients of the stress tensor

A classical experiment by means of the oblique incidence method is carried out in a transmission polariscope. If we want to achieve the interpretation of the photoelastic effects observed in the transmission polariscope, formula (2.10) must be presented in the following form

$$\frac{\lambda}{2\pi C_\sigma}\int\limits_{A_k}^{B_k}\Big[d\psi_k - \Big(\frac{a_k}{b_k}-\frac{b_k}{a_k}\Big)\sin\psi_k d\alpha_k\Big] = \int\limits_{A_k}^{B_k}(\sigma_1^{(k)}-\sigma_2^{(k)})dx_k \tag{4.1}$$

where: $A_k$, $B_k$ – points of entry and exit of light in the model, respectively. Practically this method is limited to solving a particular case, that is a problem of plane stress state (unknowns $\sigma_x$, $\sigma_y$, $\tau_{xy}$ (1.1)).

Measurement of the light field coefficients running normally and obliquely ($k = 1,2$) to the flat model was suggested for the first time by Drucker D.C. [1]. Two obtained equations (4.1), for $k = 1,2$, completed with isoclinic line parameters give the possibility of calculating the unknown variables. In works developing the metod (cf [3],[5]) the authors suggest taking measurements for three light courses ($k = 1,2,3$) to complete data for writing three independent equations (4.1). It allows us to solve the plane problem without recording isoclinic lines.

In the transmission polariscope we get the integrated value of birefringence on the geometrical path of light, what may be a source of errors, estimation of which can be difficult because of unacquaintance with the distribution of birefringence function in the direction of the light course.

It is possible to avoid errors of the method when we observe the scattered light.

Combination of the oblique incidence method with the observation of scattered light was performed by Bateson and all [6] for solving plane problems. These solutions demand for completing data with the measurement of isoclinic parameters in terms of a conventional method.

The analysis of the stress state with the aid of the oblique incidence method using only a difference of phases of component waves together with the scattered light recording is worth notice. This trend of research allows for more general analysis of the stress state in photoelastic media.

## 5. Oblique incidence method in three–dimensional conditions

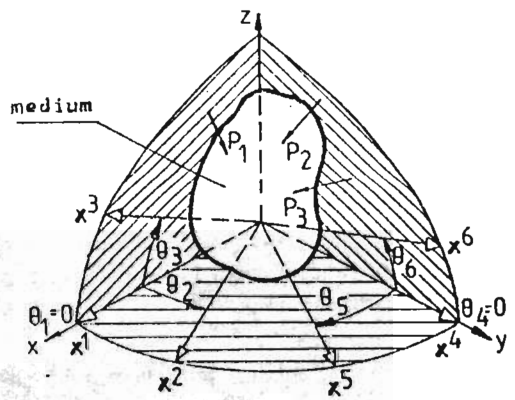


Fig. 2. Geometry of the temporary birefringence measurement. $x_{(k)}$ – directions of the light runing throught the model, $(x, y, z)$ – co-coordinate system related to examined point, $P_1, P_2, P_3, \ldots$ – loading system, $\Theta_k$ – angles refering directions $x_{(k)}$ to the $x, y, z$ system

Let us assume the system $(x, y, z)$ at the measuring point in an optional photoelastic medium, on the geometrical path of light. The oblique incidence will be considered with respect to the assumed coordinate system $(x, y, z)$, (Fig.2). Geometry of the measurement of birefringence is a more general principle of oblique incidence than the one suggested previously [5].

We induce the course of light in the direction $x_k$ $(k = 1, ..., 6)$, (Fig.2).

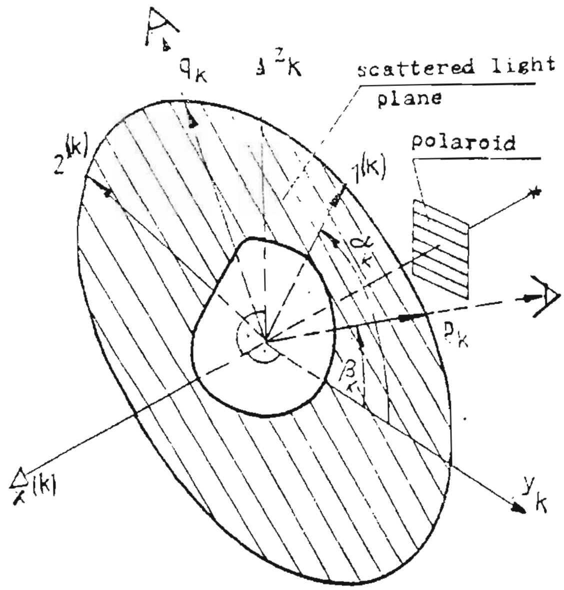


Fig. 3. Mutual position of systems connected with the polarization of falling light $(y_k, z_k)$, directions of stresses optically active $(1^{(k)}, 2^{(k)})$ and directions of observations $(p_k, q_k)$

At the measuring point, basing on the plane $\varphi = 90^o$ (3.5), three rectangular coordinate systems will be defined:
the system $(x_k, y_k, z_k)$ connected with the direction of the course and polarization of light, the system $(1^{(k)}, 2^{(k)}, 3^{(k)})$ connected with the direction of stresses optically active and the system $(p_k, q_k)$ connected with the directions of observations. Let us assume the angle $\alpha_k$ between the systems $(y_k, z_k)$ and $(1^{(k)}, 2^{(k)})$ and the angle $\beta_k$ between the systems $(p_k, q_k)$, (Fig.3).

Let the resultant of the electric field intensity vector reaching the measuring point overlap the axis $y_k$. The light field in the measuring point will be described by the expression [4,15,16]

$$\begin{bmatrix} 1 & 0 \\ 0 & e^{-i\psi_k} \end{bmatrix} \begin{bmatrix} \cos\alpha_k & -\sin\alpha_k \\ \sin\alpha_k & \cos\alpha_k \end{bmatrix}. \tag{5.1}$$

Passing to the system $(p_k, q_k)$ we will use the matrix

$$\begin{bmatrix} \cos(\alpha_k - \beta_k) & \sin(\alpha_k - \beta_k) \\ -\sin(\alpha_k - \beta_k) & \cos(\alpha_k - \beta_k) \end{bmatrix}. \tag{5.2}$$

Components of electric field intensity vector in the system $(p_k, q_k)$ will be determined by the product

$$\begin{bmatrix} \cos(\alpha_k - \beta_k) & \sin(\alpha_k - \beta_k) \\ -\sin(\alpha_k - \beta_k) & \cos(\alpha_k - \beta_k) \end{bmatrix} \begin{bmatrix} 1 & 0 \\ 0 & e^{-i\psi_k} \end{bmatrix} \cdot$$
$$\cdot \begin{bmatrix} \cos\alpha_k & -\sin\alpha_k \\ \sin\alpha_k & \cos\alpha_k \end{bmatrix} \begin{bmatrix} E_{y_k} \\ 0 \end{bmatrix} = \begin{bmatrix} E_{p_k} \\ E_{q_k} \end{bmatrix}. \tag{5.3}$$

Multiplying matrices occuring in the formula (3.4) step by step we will get

$$\begin{bmatrix} E_{y_k}\cos(\alpha_k - \beta_k)\cos\alpha_k & E_{y_k}\sin(\alpha_k - \beta_k)\sin\alpha_k e^{-i\psi_k} \\ E_{y_k}\sin(\alpha_k - \beta_k)\cos\alpha_k & -E_{y_k}\cos(\alpha_k - \beta_k)\sin\alpha_k e^{-i\psi_k} \end{bmatrix} = \begin{bmatrix} E_{q_k} \\ E_{p_k} \end{bmatrix}. \tag{5.4}$$

After multiplying components $E_{p_k}$ and $E_{q_k}$ by their complex conjugate values $E^*_{p_k}$ and $E^*_{q_k}$ we will get formulas for the scattered light intensity for observations along the directions $p_k$ and $q_k$

$$\begin{aligned} J_{p_k} &= KE_{p_k}E^*_{p_k} = KE^2_{y_k}[\sin^2\beta_k + \sin 2\alpha_k \sin 2(\alpha_k - \beta_k)(1 - \cos\psi_k)] \\ J_{q_k} &= KE_{q_k}E^*_{q_k} = KE^2_{y_k}[\cos^2\beta_k - \sin 2\alpha_k \sin 2(\alpha_k - \beta_k)(1 - \cos\psi_k)] \end{aligned} \tag{5.5}$$

where $K$ – constant depending on scattering properties of the medium. In equations (5.5) values of $\alpha_k$ and $\psi_k$ are measured. We started the observation of the scattered light on the ridge of the model where the direction of the falling light beam polarization fixes also the direction of the resultant vector of the light field. When $\beta_k = 0$ (Fig.3), the equations (5.5) have the form

$$\begin{aligned} J_{p_k} &= KE^2_{y_k}\sin^2 2\alpha_k(1 - \cos\psi_k) \\ J_{q_k} &= KE^2_{y_k}[1 - \sin^2 2\alpha_k(1 - \cos\psi_k)]. \end{aligned} \tag{5.6}$$

Rotating then the model about the $x^{(k)}$ axis we will determine its position in which

$$J_{p_k} = 0, \qquad J_{q_k} = J_{max} \tag{5.7}$$

independently from $\psi_k$.

This condition will be satisfied when $\alpha_k = 0$ and thus the quasi–principal directions, we are looking for, will overlap the directions of observations of the scattered light. Each change in $J_{p_k}$ and $J_{q_k}$ for the model placed in such a way with respect to the extreme values on the path of the light beam is associated with the change of direction $(1^{(k)}, (2^{(k)})$. This quasi–principal directions in successive points on the path of the light beam will be determined by turning the model till the conditions (5.7) are fulfilled.

The values $\psi_k$ are measured next. The model is turned from the fixed position in such a way that

$$J_{p_k} = 0 \qquad J_{q_k} = J_{max} \quad \text{when} \quad \psi_k = 2\pi m_k$$
$$J_{p_k} = J_{max} \qquad J_{q_k} = 0 \quad \text{when} \quad \psi_k = \pi m_k \tag{5.8}$$
$$m_k = 0, 1, 2, ...$$

These conditions will be satisfied when the angle $\alpha_k$ between the vector of electric field intensity and the quasi-principle direction $(1^{(k)})$ to will be equal to 45° (Fig.3). $J_{p_k}$ and $J_{q_k}$ will be then only the function of $\psi_k$

$$J_{p_k} = KE_{y_k}(1 - \cos\psi_k)$$
$$J_{q_k} = KE_{y_k}\cos\psi_k \tag{5.9}$$

and that is why we can reveal the points in which values (5.8) are known.

Putting the compensator at the entrace of light to the model allows us to state whether the acquired extreme values of the light intensity depend or not on values of $\psi_k$ and whether at the same time the quasi-principal stresses (5.7) or the phase difference of component waves (5.8) have been revealed.

Values of $\alpha_k$, $\psi_k$ denote measuring data appearing on the left side of the formula (2.10).

The system $(x_k, y_k, z_k)$, in which the parameters of the light fields are measured, is the initial system in the analysis of the right-hand side of the equation (2.10). Tensor $\sigma_{ij}$ satisfies the law of transformation and the quasi-principal stresses $\sigma_1^{(k)}$, $\sigma_2^{(k)}$, $\sigma_3^{(k)}$ (2.2) can be calculated from the formula

$$\sigma_{ij} = a_{ir}a_{js}\sigma_{rs} \tag{5.10}$$

using the function extremum conditions

$$\frac{\partial\sigma'_y}{\partial\chi} = 0, \qquad \frac{\partial\sigma'_z}{\partial\chi} = 0 \tag{5.11}$$

where

$\sigma_{rs}$ – stresses in the system $(x_k, y_k, z_k)$,

$a_{ir}$, $a_{js}$ – transformation coefficients described by the table

| | $x_k$ | $y_k$ | $z_k$ |
|---|---|---|---|
| $3^{(k)} = x'$ | 1 | 0 | 0 |
| $y'$ | 0 | $\cos\chi$ | $\sin\chi$ |
| $z'$ | 0 | $-\sin\chi$ | $\cos\chi$ |

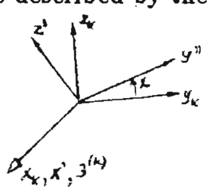

where $\chi$ – angle between the systems $(x_k, y_k, z_k)$ and $(x', y', z')$.

Performing the above operations, after elimination of the angle $\chi$ we finally get

$$\begin{aligned} \sigma_1^{(k)} &= \frac{1}{2}(\sigma_{y_k} + \sigma_{z_k}) + \frac{1}{2}\left[(\sigma_{y_k} - \sigma_{zk})^2 + 4\tau_{y_k z_k}^2\right]^{\frac{1}{2}} \\ \sigma_2^{(k)} &= \frac{1}{2}(\sigma_{y_k} + \sigma_{z_k}) - \frac{1}{2}\left[(\sigma_{y_k} - \sigma_{z_k}) + 4\tau_{y_k z_k}\right]^{\frac{1}{2}} \\ \sigma_3^{(k)} &= \sigma_{x_k}. \end{aligned} \tag{5.12}$$

On the basis of (5.12) we calculate

$$(\sigma_1^{(k)} - \sigma_2^{(k)}) = \left[(\sigma_{y_k} - \sigma_{zk})^2 + 4\tau_{y_k z_k}\right]^{\frac{1}{2}}. \tag{5.13}$$

Combining (2.10) and (5.13) for $k = 6$ we get a system of six equations expressing the relation between the stress tensor coefficients (1.1) and coefficients of the light field running through the tested medium in directions $x^{(1)},...,x^{(6)}$ (Fig.2)

$$\frac{\lambda}{2\pi C_\sigma}\left[\frac{d\psi_k}{dx_k} - \left(\frac{a_k}{b_k} - \frac{b_k}{a_k}\right)\sin\psi_k\frac{d\alpha_k}{dx_k}\right] = \left[(\sigma_{y_k} - \sigma_{z_k})^2 + 4\tau_{y_k z_k}^2\right]^{\frac{1}{2}}. \tag{5.14}$$

Limiting the analysis to the points in which $J_{p_k} = 0$, $J_{q_k} = J_{max}$ we find the values of $\psi_k = 2\pi m_k$, $\frac{d\psi_k}{dx_k} = 2\pi\frac{dm_k}{dx_k}$ formulas (5.14) are simplified then to the form

$$S_\sigma\frac{dm_k}{dx_k} = \left[(\sigma_{y_k} - \sigma_{zk})^2 + 4\tau_{y_k z_k}^2\right]^{\frac{1}{2}} \tag{5.15}$$

where $S_\sigma = \frac{\lambda}{C_\sigma}$ – material photoelastic constant.

Transforming stresses $\sigma_{y_k}$, $\sigma_{z_k}$, $\tau_{y_k z_k}$ to the system $(x, y, z)$ and taking into account angles $\Theta_1 = 0$, $\Theta_2$, $\Theta_3$, $\Theta_4 = 0$, $\Theta_5$, $\Theta_6$ (Fig.2), when the axis $x$ overlaps the direction $x^{(1)}$ and the axis $y$ overlaps the direction $x^{(4)}$, we finally get for the succesive directions $x^{(1)},...,x^{(6)}$

$$\begin{aligned} S_\sigma\frac{dm_1}{dx_1} &= \left[(\sigma_y - \sigma_z)^2 + 4\tau_{yz}^2\right]^{\frac{1}{2}} \\ S_\sigma\frac{dm_2}{dx_2} &= \Big[(\sigma_x\sin^2\Theta_2 + \sigma_y\cos^2\Theta_2 - 2\tau_{xy}\sin\Theta_2\cos\Theta_2 - \sigma_z)^2 + \\ &+ 4(\tau_{yz}\cos\Theta_2 - \tau_{zx}\sin\Theta_2)^2\Big]^{\frac{1}{2}} \\ S_\sigma\frac{dm_3}{dx_3} &= \Big[(\sigma_y - \sigma_x\sin^2\Theta_3 - \sigma_z\cos^2\Theta_3 - 2\tau_{zx}\cos\Theta_3\sin\Theta_3)^2 + \\ &+ 4(-\tau_{xy}\sin\Theta_3 + \tau_{yz}\cos\Theta_3)^2\Big]^{\frac{1}{2}} \\ S_\sigma\frac{dm_4}{dx_4} &= \left[(\sigma_z - \sigma_x)^2 + 4\tau_{zx}^2\right]^{\frac{1}{2}} \end{aligned} \tag{5.16}$$

$$S_\sigma \frac{dm_5}{dx_5} = \Big[(\sigma_y \sin^2\Theta_5 + \sigma_z \cos^2\Theta_5 - 2\tau_{yz}\sin\Theta_5\cos\Theta_5 - \sigma_x)^2 + $$
$$+ \; 4(-\tau_{xy}\sin\Theta_5 + \tau_{zx}\cos\Theta_5)^2\Big]^{\frac{1}{2}}$$
$$S_\sigma \frac{dm_6}{dx_6} = \Big[(\sigma_z - \sigma_x \cos^2\Theta_6 - \sigma_y \sin^2\Theta_6 - 2\tau_{xy}\cos\Theta_6\sin\Theta_6)^2 + $$
$$+ \; 4(\tau_{yz}\sin\Theta_6 + \tau_{zx}\cos\Theta_6)^2\Big]^{\frac{1}{2}}.$$

On the geometrical path $x^{(k)}$ of the light running through the photoelastic medium, from the point of entry of light into the model, to the point in which the light leaves the model, values of $m_k$ ($m_k = 0, 1, 2, ...$) must be assigned to successively appearing places in which $J_{p_k} = 0$, $J_{q_k} = J_{max}$. It will let us to determine the relation between $m_k(x_k)$ and $\frac{dm_k(x_k)}{dx_k}$ and the sought–after system of quations.

## References


1. DRUCKER D.C., *Photoelastic Separation of Principal Stresses by Oblique Incidence,* J.Appl.Mech., Trans.AMME, 65, A 156-160, 1943
2. JESSOP H.T., *The Scattered Light Method of Exploration of Sresses in Two- and Three-dimensional Models,* British J.of Appl.Physics, vol 2, 1951
3. NORRIS C.B., VOSS A.W., *An Improved Photoelastic Method for Determining Plane Stress,* NACATN 1410, January 1948
4. KOMOROWSKI J., STUPNICKI J., *Strain Measurement with Asymmetric Oblique–incidence Polariscope for Birefringent Coatings,* Exp.Mech., 1983
5. SIKOŃ M., *Metoda skośnego prześwietlania do analizy płaskiego stanu naprężenia przy wykorzystaniu jedynie pola izochrom,* Mech.Teoret.i Stos., 1, 27, 1989
6. BATESON S., HUNT J.W., DALBY D.A., SINHA N.K., *Stress measurements in tempered glass plates by scattered light method with a laser source,* Bull.Am.Ceram. Soc., 45, 1, 1966
7. DRUCKER D.C., *The method of oblique incidence in photoelasticy,* Proc.SESA, XII, 56-66, 1955
8. KOMOROWSKI J., AND STUPNICKI J., *Sources of Error in Oblique–incidence Photo–stress method,* Proc.IUTAM Symp. on Optical Methods in Mechanics of Solids, 1979, Poitiers, Sijthoff Noordhoff 1981
9. ALISSON J.M., *Least Squares Solution of the Oblique–incidence Equations,* VDI Berichte Nr 102, 1966
10. HUNG Y.Y., POTTINGER M.G., *An Improved Oblique–incidence Technique for Principal-strain Separation in Photoelastic Coatings,* Exp.Mech., May 1980
11. PINDERA J.T., STRAKA P., *Response of the Integrated Polariscope,* J.of Strain Anal., 8, no.1, 1973

12. SRINATH L.S., FROCHT M.M., *Scattered light in photoelasticity*, Exp.Mech., Oct. 1989

13. SRINATH L.S., *Analysis of Scattered-light method in photoelasticity*, Exp.Mech., Oct. 1969

14. CHENG Y.F., *A scattered-light photoelastic method for the determination of tempered stresses in aircraft windhields*, Boening Sci.Res.Lab., Seattle, Washington, Apr. 1967

15. KAPKOWSKI J., SŁOWIKOWSKA I., STUPNICKI J., *Badanie naprężeń metodą elastooptycznej warstwy powierzchniowej*, PWN, Warszawa 1987

16. STUPNICKI J., *Optyczne metody badan w mechanice*, in Mech.Techniczna, tom X, PWN, Warszawa 1984

17. *Encyklopedia Fizyki*, PWN 1979



Streszczenie

W pracy sformułowano ogólne związki dla badań elastooptycznych, w formie układu równań zawierających składowe tensora naprężenia i parametry pola świetlnego przebiegającego przez badany ośrodek.
Rozważania przeprowadzone są w oparciu o metodę skośnego prześwietlania, w połączeniu z obserwacją światła rozproszonego.
W dodatku 1 zawarty jest opis płaskiej fali elektromagnetycznej w ośrodku anizotropowym. Analizę tą zaadoptowano dla potrzeb elastooptyki oraz powiązano z koncepcją naprężeń optycznie czynnych (wtórnych naprężeń głównych).
Dodatek 2 zawiera część doświadczalną pracy. Wyniki przeprowadzonego eksperymentu oraz analiza błędu dowodzą słuszności wyprowadzonych związków i uniwersalności metody.

Praca stanowi punkt wyjścia w analizie złożonych stanów naprężenia.


# 6. Appendix 1

## 6.1. Plane electromagnetic wave in photoelastic medium

Maxwell's equations of the electromagnetic theory of light for transparent anisotropic media without any electric charge and without the passage of current have the following form

$$\begin{aligned} \mathrm{rot}\boldsymbol{H} &= \frac{1}{c}\frac{\partial \boldsymbol{D}}{\partial t} \\ \mathrm{rot}\boldsymbol{E} &= -\frac{1}{c}\frac{\partial \boldsymbol{H}}{\partial t} \end{aligned} \tag{6.1}$$

where
$\boldsymbol{H}$ – magnetic intensity,
$\boldsymbol{E}$ – electric field intensity,
$\boldsymbol{D}$ – electric induction,
$c$ – speed of light in a vacuum.

Plane monochromatic wave can be presented in the form

$$\boldsymbol{E} = \boldsymbol{E}_0 \exp\Big[\mathrm{i}\omega\Big(t - \frac{\boldsymbol{\nu r}}{v} + \frac{\delta_0}{\omega}\Big)\Big] \tag{6.2}$$

where
$E_0$ – amplitude,
$\omega$ – circular wave frequency,
$t$ – time,
$\boldsymbol{\nu}$ – unit vector normal to the wave front,
$\boldsymbol{r}$ – present radius–vector of the point,
$v$ – phase velocity of the wave,
$\delta_0$ – initial phase,
i – imaginary unit, $i^2 = -1$.

Replacing $(6.1)_2$ with (6.2) we get

$$-\frac{1}{c}\frac{\partial \boldsymbol{H}}{\partial t} = \mathrm{rot}\Big\{E_0 \exp\Big[\mathrm{i}\omega\Big(t - \frac{\boldsymbol{r\nu}}{v} + \frac{\delta_0}{\omega}\Big)\Big]\Big\}. \tag{6.3}$$

For the vector $\boldsymbol{E}_0$ and the scalar $u = \exp\Big[\mathrm{i}\omega\Big(t - \frac{\boldsymbol{r\nu}}{v} + \frac{\delta_0}{\omega}\Big)\Big]$ in which $(\boldsymbol{r\nu})$ is a variable, the course will be carried out according to the formula

$$\mathrm{rot}(u\boldsymbol{E}_0) = \nabla \times (u\boldsymbol{E}_0) = u(\nabla \times \boldsymbol{E}_0) + (\nabla u) \times \boldsymbol{E} \tag{6.4}$$

where

$$\nabla = \Big[\frac{\partial}{\partial x}, \frac{\partial}{\partial y}, \frac{\partial}{\partial z}\Big].$$

For a homogenous vector field

$$\nabla \times \boldsymbol{E}_0 = \boldsymbol{0} \tag{6.5}$$

and

$$\nabla u(\boldsymbol{r\nu}) = \frac{du}{d(\boldsymbol{r\nu})}\nabla(\boldsymbol{r\nu}) \tag{6.6}$$

and the equation (6.3) will be presented in the following form

$$\frac{1}{c}\frac{\partial \boldsymbol{H}}{\partial t} = \frac{\mathrm{i}\omega}{v}\{\nabla(\boldsymbol{r\nu}) \times \boldsymbol{E}\}. \tag{6.7}$$

Since

$$\nabla(\boldsymbol{r}\boldsymbol{\nu}) = \nabla\underline{\boldsymbol{r}}\cdot\boldsymbol{\nu} + \nabla\boldsymbol{r}\cdot\underline{\boldsymbol{\nu}} = \boldsymbol{\nu} \tag{6.8}$$

we finally get

$$\frac{1}{c}\frac{\partial \boldsymbol{H}}{\partial t} = \frac{\mathrm{i}\omega}{v}(\boldsymbol{\nu}\times\boldsymbol{E}). \tag{6.9}$$

Integrating the expression (6.9) with respect to time

$$\frac{1}{c}\int\frac{\partial \boldsymbol{H}}{\partial t}dt = \frac{\mathrm{i}\omega}{v}\int\Big\{\boldsymbol{\nu}\times\boldsymbol{E}_0\exp\Big[\mathrm{i}\omega\Big(t-\frac{\boldsymbol{r}\boldsymbol{\nu}}{v}+\frac{\delta_0}{\omega}\Big)\Big]\Big\}dt \tag{6.10}$$

we will get

$$\frac{1}{c}\boldsymbol{H} = \frac{1}{v}(\boldsymbol{\nu}\times\boldsymbol{E}). \tag{6.11}$$

Similarly as in the case of the vector $\boldsymbol{E}$ (6.2), the change of the vector can be defined by the formula

$$\boldsymbol{H} = \frac{c}{v}(\boldsymbol{\nu}\times\boldsymbol{E})\exp\Big[\mathrm{i}\omega\Big(t-\frac{\boldsymbol{r}\boldsymbol{\nu}}{v}+\frac{\delta_0}{\omega}\Big)\Big] \tag{6.12}$$

what means that for the plane wave vector $\boldsymbol{H}$ changes also when $\omega$ frequency varies and is perpendicular to vectors $\boldsymbol{E}$ and $\boldsymbol{\nu}$. When we put (6.12) into the formula $(6.1)_1$ taking into consideration operations (6.4), (6.5), (6.6), (6.7) and integrating thus obtained expressions with respect to time we finally get an expression

$$\frac{1}{c}\boldsymbol{D} = -\frac{1}{v}(\boldsymbol{\nu}\times\boldsymbol{H}). \tag{6.13}$$

$\boldsymbol{H}$ calculated according to the formula (6.11) will be placed in the formula (6.13) and now

$$\boldsymbol{D} = -\frac{c^2}{v^2}[\boldsymbol{\nu}\times(\boldsymbol{\nu}\times\boldsymbol{E})]. \tag{6.14}$$

Performing an operation

$$\boldsymbol{\nu}\times(\boldsymbol{\nu}\times\boldsymbol{E}) = \boldsymbol{\nu}(\boldsymbol{\nu}\boldsymbol{E}) - \boldsymbol{E} \tag{6.15}$$

we get the expression

$$\frac{v^2}{c^2}\boldsymbol{D} - \boldsymbol{E} + \boldsymbol{\nu}(\boldsymbol{\nu}\boldsymbol{E}) = \boldsymbol{0}. \tag{6.16}$$

Now we apply the formula

$$\boldsymbol{D} = \hat{\boldsymbol{\kappa}}\boldsymbol{E} \tag{6.17}$$

where $\hat{\boldsymbol{\kappa}}$ – tensor of permittivity coefficients.

Dielectric tensor $\hat{\kappa}$ is symmetrical and it can be represented in the principal axes along which diagonal elements have the values $\kappa_1$, $\kappa_2$, $\kappa_3$, respectively

$$\hat{\kappa} = \begin{vmatrix} \kappa_1 & 0 & 0 \\ 0 & \kappa_2 & 0 \\ 0 & 0 & \kappa_3 \end{vmatrix}. \tag{6.18}$$

For principal directions formula (6.17) has the form

$$D_i = \kappa_i E_i, \qquad i = 1, 2, 3. \tag{6.19}$$

Combining (6.19) and (6.16) we can write for principal axes of the tensor $\hat{\kappa}$

$$D_i = \frac{\nu_i(\boldsymbol{\nu E})}{\frac{1}{\kappa_i} - \frac{v^2}{c^2}}. \tag{6.20}$$

It follows from (6.11) and (6.13) that $(\boldsymbol{D\nu}) = 0$ and $(\boldsymbol{E\nu}) \neq 0$, so on the basis of (6.20) we can write a formula

$$\frac{(\boldsymbol{D\nu})}{(\boldsymbol{E\nu})} = \frac{\sum_i^3 D_i\nu_i}{(\boldsymbol{E\nu})} = \frac{\nu_1^2}{\frac{1}{\kappa_1} - \frac{v^2}{c^2}} + \frac{\nu_2^2}{\frac{1}{\kappa_2} - \frac{v^2}{c^2}} + \frac{\nu_3^2}{\frac{1}{\kappa_3} - \frac{v^2}{c^2}} = 0. \tag{6.21}$$

Expression (6.21) is a quadratic equation and it generally has two solutions. Let us denote the roots of the equation (6.21) by $v'$ and $v''$. In anisotropic media, in optional direction $\boldsymbol{\nu}$, two lineary polarized waves, will propagate at different velocities $v'$ and $v''$. Let us introduce three principal velocities, $v_1$, $v_2$, $v_3$ according to the formula

$$v_i = \frac{c}{\sqrt{\kappa_i}} \tag{6.22}$$

and corresponding principal refractive indices $n_1$, $n_2$, $n_3$

$$n_i = \sqrt{\kappa_i}. \tag{6.23}$$

If $v'$ and $v''$ are velocities corresponding to $\boldsymbol{\nu}$ direction, then on the basis of (6.20) and (6.22), directions cosines of corresponding values $\boldsymbol{D}'$ and $\boldsymbol{D}''$ will be proportional to the expressions

$$\frac{\nu_i}{v_i^2 - (v')} \tag{6.24}$$

$$\frac{\nu_i}{v_i^2 - (v'')} \tag{6.25}$$

respectively.

Calculating the scalar product $D'$ and $D''$ taking into consideration (6.24), (6.25) and (6.21) we can state that

$$(D'D'') = 0. \tag{6.26}$$

It means that in the given direction $\nu$ two lineary polarized waves will propagate at $v'$ and $v''$ velocities in mutually perpendicular directions of vectors $D'$ and $D''$ (and mutually perpendicular $E'$ and $E''$).

In optically anisotropic media vectors $E$ and $D$ generally do not overlap. But in the one, examined in this work, birefringence anisotropy is small and it can be assumed that the angle between $E$ and $D$ vectors is equal to zero and, further on, it can be assumed that the normal to the light wave front overlaps the direction of the course of light $x^{(k)}$. Thus, in photoelastic media vectors $D'$ and $D''$ will correspond to the direction of the course of beams $x^{(k)}$. To determine vectors $D'$ and $D''$ optical indicatrix is used. The equation (6.2) given above describes this surface. Directions of vectors $D'$ and $D''$ (called quasiprincipal directions) overlap semi-axes of the ellipse which was formed as a result of indicatrix cross-section with the plane going through its geometrical centre and a normal to $x^{(k)}$. Stresses calculated in directions $D'$ and $D''$ are called stresses optically active or secondary principal stresses.

Since photoelastic medium satisfies the assumptions of material continuum, stresses optically active satisfy the law (6.3) given above (6.3), and coefficients $\kappa_1^{(k)}$ and $\kappa_2^{(k)}$ reach the extreme values in quasi-principal directions $(1^{(k)})$, $(2^{(k)})$ stresses $\sigma_1^{(k)}$, $\sigma_2^{(k)}$ are determined as extreme normal stresses in the cross-section perpendicular to $x^{(k)}$.

## References


1. GORSZKOW M.M., *Elipsometria,* Moskva, Sowetskoje Radio, 1974
2. BORN M., WOLF R., *Principles of Optics,* Pergamon Press 1975
3. *Poradnik Inżyniera, Matematyka,* WNT, Warszawa 1971


## 7. Appendix 2

In the first step the mathematical relations being obtained (eq (5.16)) were experimentally tested for a known case of a flat disk under the action of two concentrated forces. Knowing the stress state distribution in a chosen model makes it possible to evaluate the state of correctness of the suggested method.

In the case of the flat stress state and the course of light through the model in directions $x^{(1)}$, $x^{(2)}$, $x^{(3)}$ (Fig.2), equations (5.16) simplify to the following form

$$
\begin{aligned}
S_\sigma \frac{dm_1}{dx_1} &= \sigma_y \\
S_\sigma \frac{dm_2}{dx_2} &= \sigma_x \sin^2 \Theta_2 + \sigma_y \cos^2 \Theta_2 - \tau_{xy} \sin 2\Theta_2 \\
S_\sigma \frac{dm_3}{dx_3} &= \left[(\sigma_y - \sigma_x \sin^2 \Theta_3)^2 + 4\tau_{xy}^2 \sin^2 \Theta_3\right]^{\frac{1}{2}}.
\end{aligned}
\tag{7.1}
$$

The plane stress state is realized on a disk made of exposide resin ($S_\sigma = 6.5 \cdot 10^{-4}$ [MN/order]) of a diameter $d = 0.062$ [m] and thickness $g = 0.0318$ [m], under concentrated forces $P = 80$ [N].

Under the forces action, constant optical anisotropy of the model was introduced by means of the stress freezing technique.

Since the birefringence measurement are limited to the points lying on a diameter perpendicular to the direction of the force, where $\sigma_y = \sigma_2$, $\tau_{xy} = 0$ ($\sigma_1$, $\sigma_2$ – principal stresses), equations (7.1) simplifity to the following form

$$
\begin{aligned}
S_\sigma \frac{dm_1}{dx_1} &= \sigma_2 \\
S_\sigma \frac{dm_2}{dx_2} &= \sigma_1 \sin^2 \Theta_2 + \sigma_2 \cos^2 \Theta_2 \\
S_\sigma \frac{dm_3}{dx_3} &= \sigma_2 - \sigma_1 \sin^2 \Theta_3.
\end{aligned}
\tag{7.2}
$$

From the system (7.2) we get

$$
\begin{aligned}
\sigma_2 &= S_\sigma \frac{dm_1}{dx_1} \\
\sigma_1^{(2)} &= \frac{S_\sigma}{\sin^2 \Theta_2}\Big(\frac{dm_2}{dx_2} - \frac{dm_1}{dx_1} \cos^2 \Theta_2\Big) \\
\sigma_1^{(3)} &= \frac{S_\sigma}{\sin^2 \Theta_3}\Big(\frac{dm_1}{dx_1} - \frac{dm_3}{dx_3}\Big)
\end{aligned}
\tag{7.3}
$$

where $\sigma_1^{(2)}$, $\sigma_1^{(3)}$ – denotes stresses determined when light goes in directions $x^{(2)}$ and $x^{(3)}$.

A diagram of measuring position is shown in Fig.4. The source of light (laser He–Ne 0.1 [mw] power) moves in a horizontal plane. This movement is possible through a feed screw driven by an electric motor. Belt transmission put between the motor and the feed screw causes the speed of laser movement equal to 10 [mm/min]. On the path of the light beam, on the outrigger fixed to the laser casing a polaroid and a compensator are placed. The light goes then to a vessel.

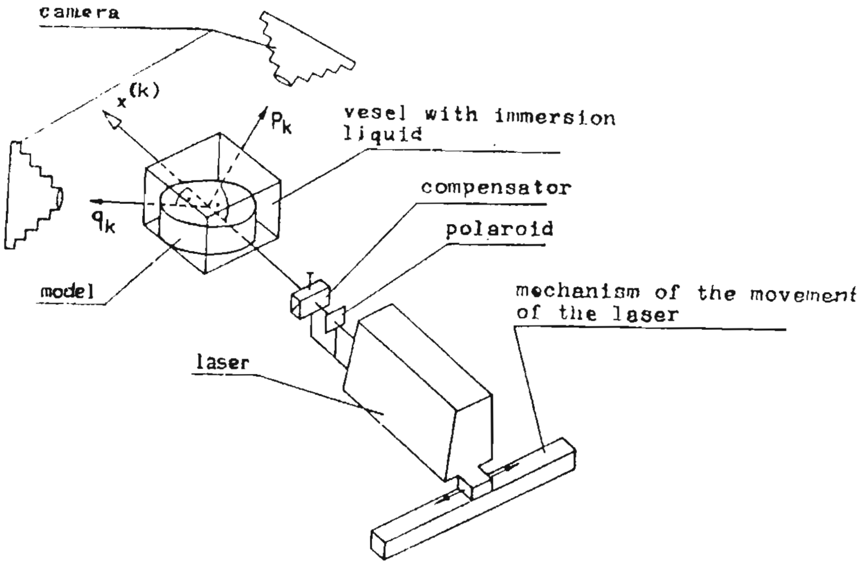


Fig. 4. Diagram of the measuring position

A camera recording birefringence effect is fixed to the stand on the scattering plane.

Fig.5 shows an idea of optical effects recording according to the theory presented in the paper. (For easier presentation of the position of the model in the space with respect to the light source and recording system, a plane disk has been inscribed onto a sphere). Three figures a), b), c) present three different positions of the model for the course of light in the directions $x^{(k}$, $(k = 1,2,3)$. In these figures systems $(x,y,z)$, $(1^{(k)},2^{(k)},3^{(k)})$, $(x_k,y_k,z_k)$, $(p_k,q_k)$ and angles $\alpha_k$, $\beta_k$, $\Theta_k$, are denoted according to the marking system introduced in the theoretical part of this paper. Besides, several elements were marked: $E_{y_k}$ – electric field intensity vector, $-Y_1+Y_1$, $-Y_2+Y_2$, $-Z_3+Z_3$ – directions of light source movement at the moment of measurement recording, $P$ – forces acting on the model, scattering planes and measuring surfaces. In sections of the model, lined up in Fig.5, optical effects are recorded on a light–sensitive plate during the movement of the light source at the opened camera lens. The direction of the course of light is determined in such a way that $\Theta_1 = 0$, $\Theta_2 = \Theta_3 = 45^o$ (Fig.1) and $\alpha_k = 45^o$ i $\beta_k = 0^o$.

Results of experiments, have been gathered in Fig.6. On photos the coordinate system $(x,y)$ and directions of the course of light $x^{(1)}$, $x^{(2)}$, $x^{(3)}$ are marked. Figures 6.1a,b,c present optical effects observed in the direction $p_k$, and Fig.6.2a,b,c optical picture recorded when the axis of the camera is in line with the direction $q_k$.

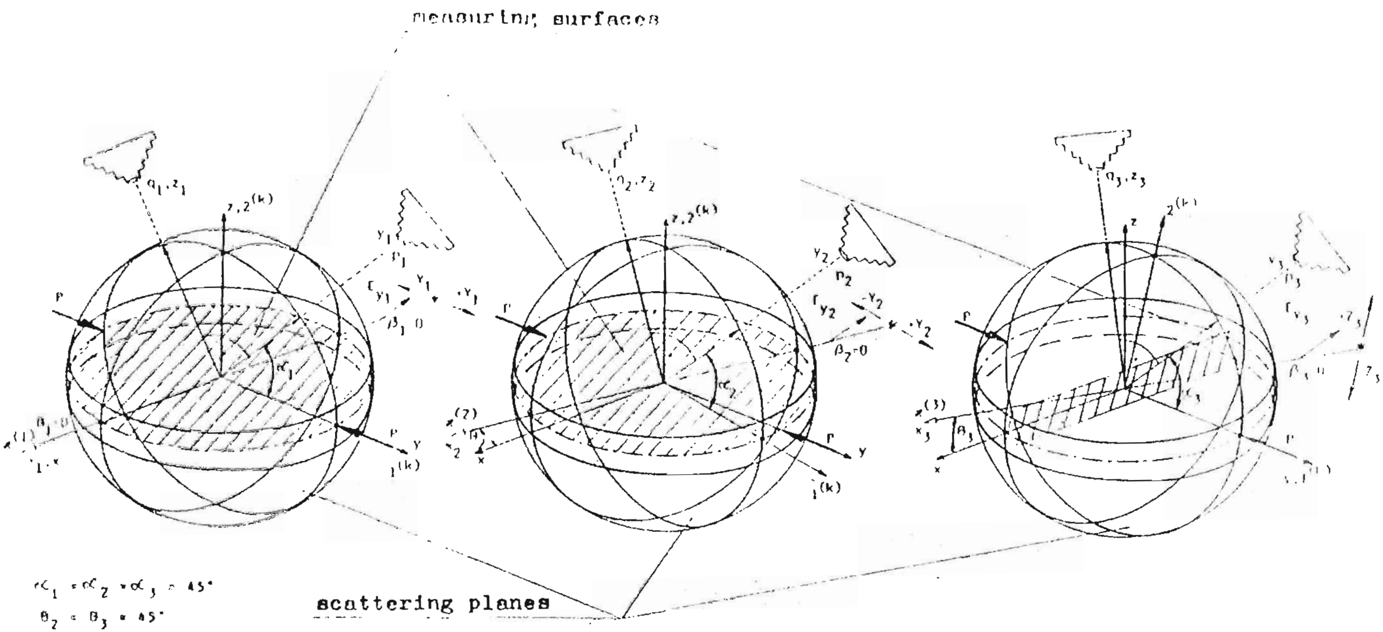


**Fig. 5.** Conditions of the light running through the model and registration of optical effects

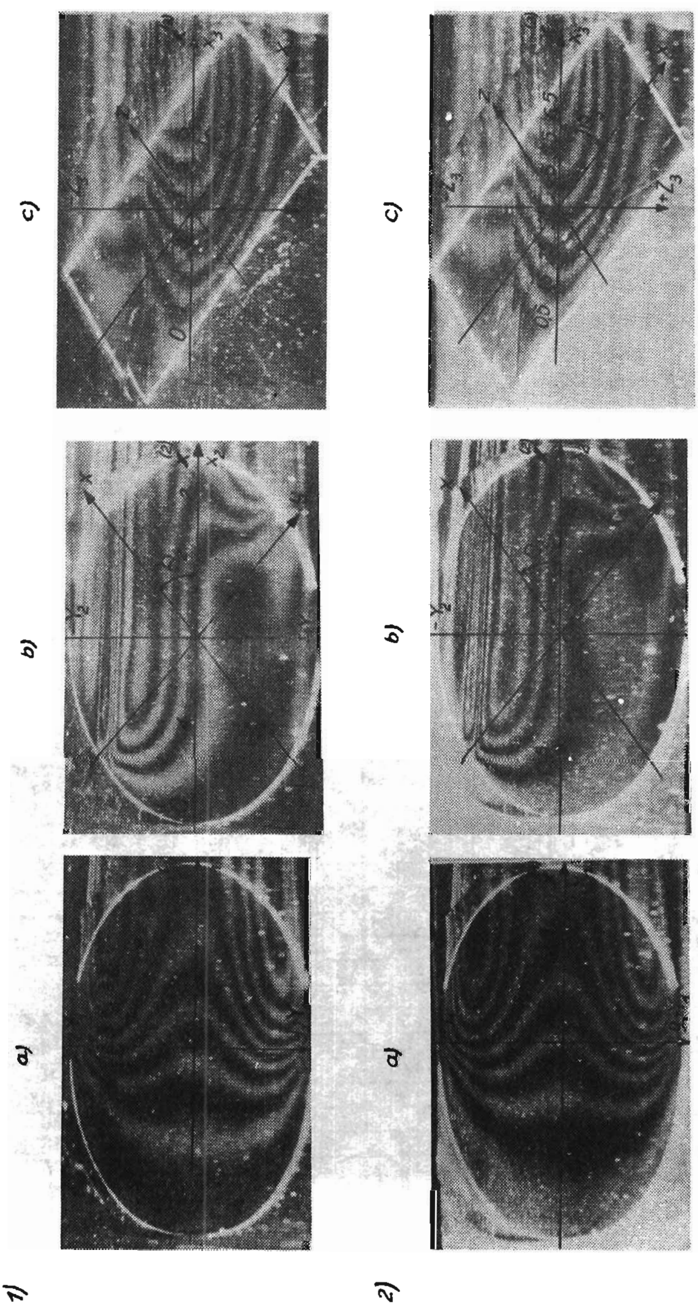


Fig. 6. Results of experiments in photographic form. Light coming a) normally, b)c) obliquelly in relation to $(x, y, z)$ system camera is placed longways 1) $p_n$, 2) $q_n$ direction (Fig.5)

Measuring points are denoted in figures by $m = 0, 1, 2, ...$ or $m = 0.5; 1.5; 2.5, ...$ on the places appearing successively on the axis $x_k$ for which $J_{p_k} = 0$ or $J_{q_k} = 0$ (Fig.6.1a,b,c and 6.2a,b,c). Measuring points become a basis for diagrams $m_k(x_k)$ (Fig.7,8,9) and on this basis, by means of graphic differentiation $dm_k(x_k)/dx_k$ was determined. Fig.7 contains measuring data $m_1(x_1)$ and the result of graphic differentiation $dm_1(x_1)/dx_1$ for all measuring points since the axis $x_1$ (direction of the course of light) and the axis $x$ on which measuring points are located, mutually overlap. If we want to find the values of $dm_2/dx_2$ and $dm_3/dx_3$ it is necessary to draw axes $x_2$ and $x_3$ through measuring points, draw then the diagrams $m_2(x_2)$ and $m_3(x_3)$ and determine the derivatives $dm_2/dx_2$, $dm_3/dx_3$ in the measuring points.

Such operations are performed in Fig.8 and 9 for points of coordinate axes $x = -0.015$ [m] and $x = 0.015$ [m] as an example. The next phase is the estimation of derivative characters $dm_k/dx_k$ ($k = 1, 2, 3$). If $m_k > 0$ than the value of $dm_k/dx_k$ depends on function monotony $m_k(x_k)$. This property can be evaluated by means of a compensator. At the entrance into the model the compensator introduces a known fractional value $\Delta m_k$. When $\Delta m_k > 0$ and the function $m_k(x_k)$ is monotonically increasing the points $J_{p_k} = 0$ or $J_{q_k} = 0$ will be moved in the positive direction of the axis $x_k$ ($dm_k/dx_k > 0$), when the function is monotonically decreasing then the displacement is perfomed in the negative direction of the axis $x_k$ ($dm_k/dx_k < 0$). After the experiment with the use of the compensator values of $dm_k/dx_k$ were marked and put into the table 1.

**Table 1.** Results of experiments. $\sigma_{1t}$, $\sigma_{2t}$ – stresses obtained according to the theoretical formulas, $\sigma_1$, $\sigma_2$ – stresses calculated experimentaly, $dm_1/dx_1$, $dm_2/dx_2$, $dm_3/dx_3$ – values received with the aid of graphic differentiation of the function $m_1(x_1)$, $m_2(x_2)$, $m_3(x_3)$.

| | $x \cdot 10^{-3}$ [m] | $\sigma_{1t} \cdot 10^{-2}$ $\left[\frac{MN}{m^2}\right]$ | $\sigma_{2t} \cdot 10^{-2}$ $\left[\frac{MN}{m^2}\right]$ | $\frac{dm_1}{dx_1}$ $\left[\frac{order}{m}\right]$ | $\sigma_2 \cdot 10^{-3}$ $\left[\frac{MN}{m^2}\right]$ | $\frac{dm_2}{dx_2}$ $\left[\frac{order}{m}\right]$ | $\sigma_1^{(2)} \cdot 10^{-3}$ $\left[\frac{MN}{m^2}\right]$ | $\frac{dm_3}{dx_3}$ $\left[\frac{order}{m}\right]$ | $\sigma_1^{(3)} \cdot 10^{-3}$ $\left[\frac{MN}{m^2}\right]$ |
|---|---|---|---|---|---|---|---|---|---|
| 1 | -30 | 0.01 | -0.34 | -5 | -0.32 | | | | |
| 2 | -25 | 0.15 | -1.40 | -21 | -1.37 | -9.5 | 0.13 | | |
| 3 | -20 | 0.49 | -2.76 | -41 | -2.67 | -17 | 0.55 | | |
| 4 | -15 | 1.06 | -4.36 | -67 | -4.36 | -25 | 1.11 | | |
| 5 | -10 | 1.74 | -5.99 | -93 | -6.05 | -32 | 1.89 | | |
| 6 | -5 | 2.58 | -7.27 | -112 | -7.28 | -35 | 2.73 | | |
| 7 | 0 | 2.58 | -7.75 | -119 | -7.73 | -36 | 3.06 | -138 | 2.47 |
| 8 | 5 | 2.58 | -7.27 | -119 | -7.28 | | | -128 | 2.08 |
| 9 | 10 | 1.74 | -5.99 | -93 | -6.05 | | | -106 | 1.69 |
| 10 | 15 | 1.06 | -4.36 | -67 | -4.36 | | | -74 | 0.91 |
| 11 | 20 | 0.49 | -2.76 | -41 | -2.67 | | | -46 | 0.65 |
| 12 | 25 | 0.15 | -1.40 | -21 | -1.37 | | | -22 | 0.13 |
| 13 | 30 | 0.01 | -0.34 | -5 | -0.32 | | | -5.5 | 0.07 |

Introduction of the fractional value $\Delta m_k$ at the entrance into the model gives us the possibility of revealing additional points of a known difference of phases

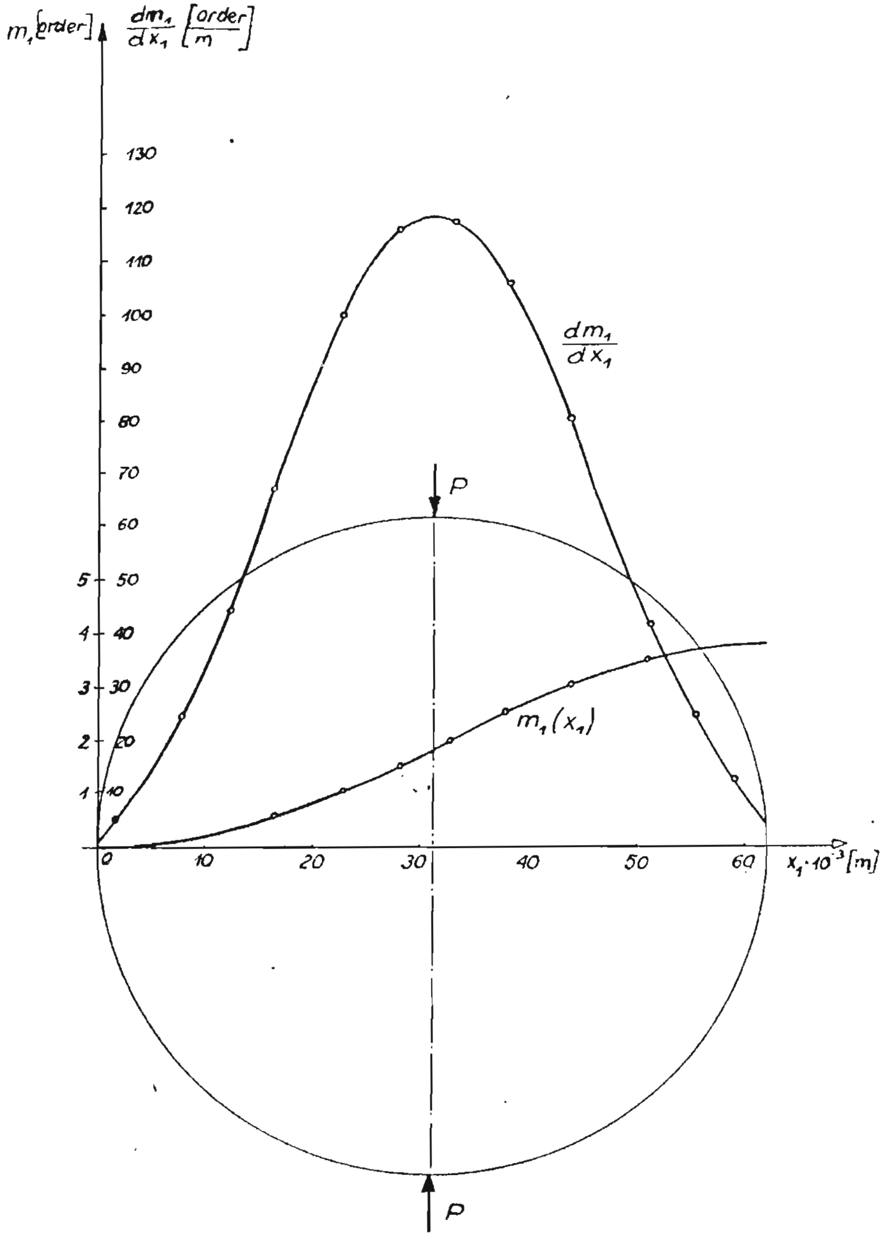


Fig. 7. Variation of $m_1$ versus $x_1$ drawn on the basis of pictures (Fig.6) and the variation of $dm_1/dx_1$ being result of graphic differentiation of the function $m_1(x_1)$

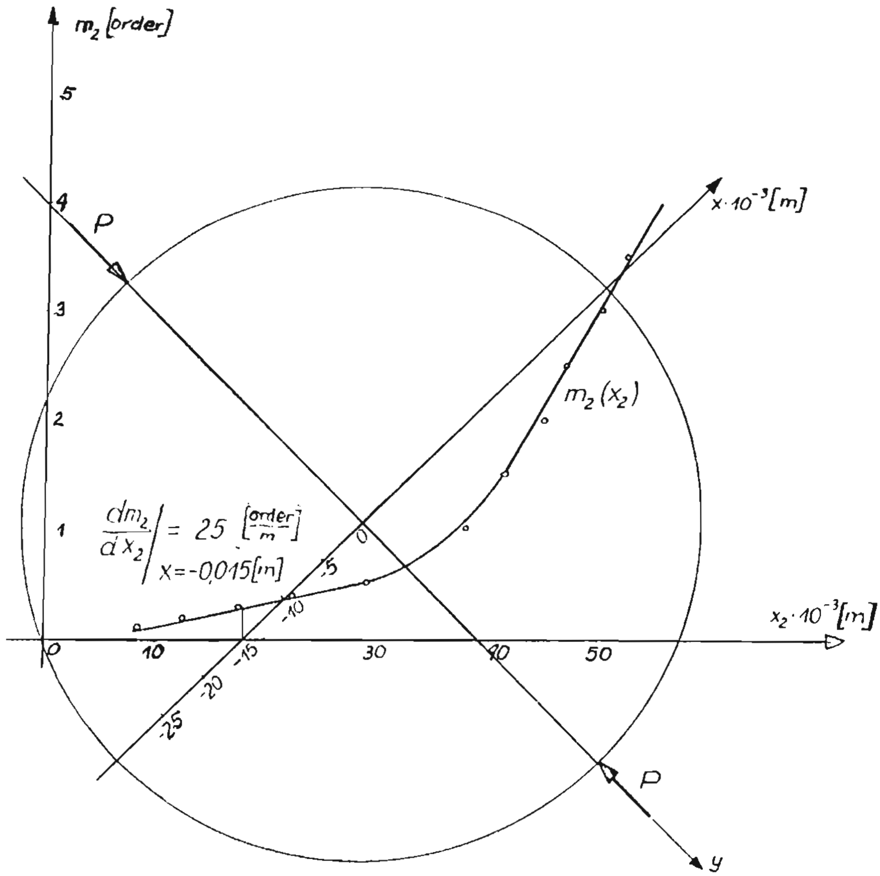


Fig. 8. Variation of $m_2$ versus $x_2$ drawn on the basis of Fig.5

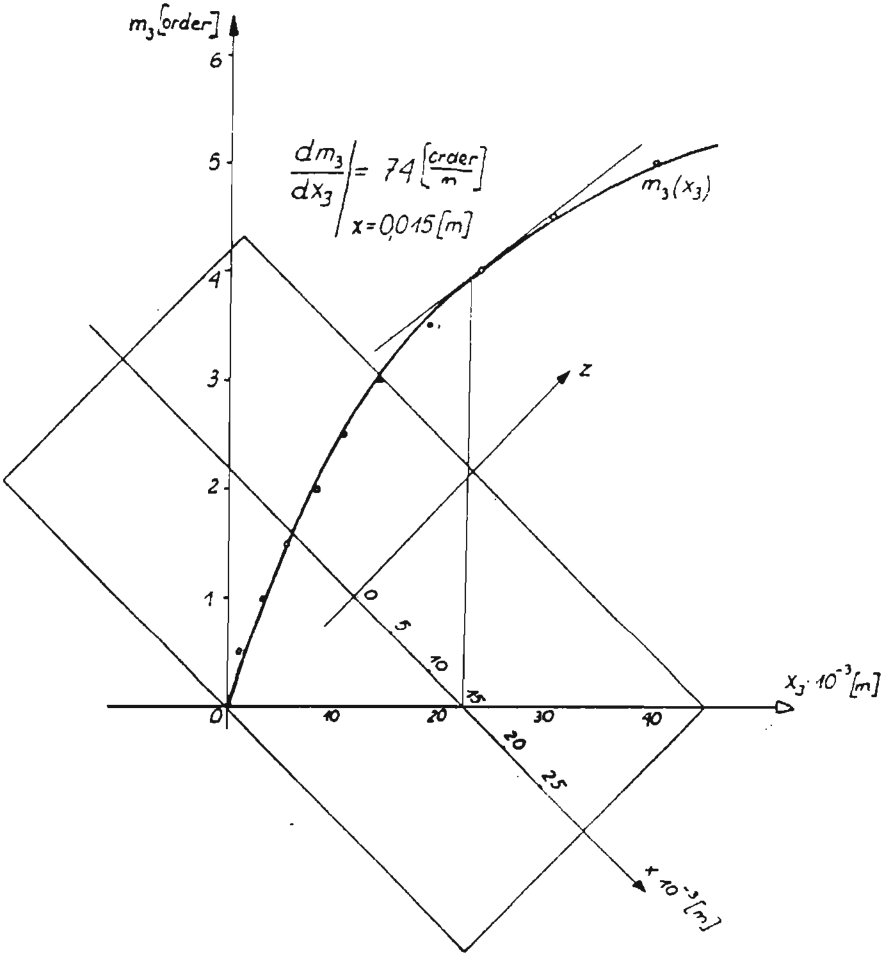


Fig. 9. Variation of $m_3$ versus $x_3$

between component waves. Scattered light intensity has the following form

$$J^0_{p_k} = KE^2_{y_k}[1 - \cos(\psi_k + \Delta\psi_k)]$$
$$J^0_{q_k} = KE^2_{y_k}\cos(\psi_k + \Delta\psi_k) \tag{7.4}$$

where $\Delta\psi_k$ – fractional value of relative retardation introduced by the compensator.

Fractional values of phase difference $\psi_k + \Delta\psi_k = 2\pi(m_k + \Delta m_k)$ appear in places on the axis $x_k$, for which $J^0_{p_k} = 0$ and $J^0_{p_k} = J_{max}$. Results of measurement of birefringence with the use of a compensator are given in table 2.

**Table 2.** Assignement of points of coordinate $x_2$ to the values $m_2$ given by the compensator.

| $\Delta m_2$ [order] | $x_2 \cdot 10^{-3}$ [m] |
|---|---|
| 0.1 | 8.5 |
| 0.2 | 15 |
| 0.3 | 18 |
| 0.4 | 22.5 |
| 0.5 | 29 |

Values $\Delta m_2$ set by the compensator correspond to the places of $x_2$ coordinates for which $Jp_2 = 0$. The obtained values were as a complementary data used to draw the diagram $m_2(x_2)$, (Fig.8). On the basis of the obtained data, using formulas (7.4) stresses were determined. The sought–after stresses were also calculated on the basis of theoretical formulae

$$\sigma_{1t} = \frac{2P}{\pi g d}\Big[1 - \frac{4x^2R^2}{(x^2+R^2)^2}\Big]$$
$$\sigma_{2t} = \frac{2P}{\pi g d}\Big[1 - \frac{4R^4}{(x^2+R^2)^2}\Big]. \tag{7.5}$$

Results are in table 1.

Diagrams of stresses determined experimentally and theoretically are in Fig.10.

Values of stresses calculated on the basis of experimental data reveal an error which depends, first of all, on the accuracy of calculated derivatives $dm_k/dx_k$ ($k = 1,2,3$), and on the precision of locating the model towards the light source (angle $\Theta_k$). Derivatives $dm_k/dx_k$ are calculated with the aid of the differential quotient

$$\frac{dm_k}{dx_k} = \frac{\Delta m_k}{\Delta x_k}. \tag{7.6}$$

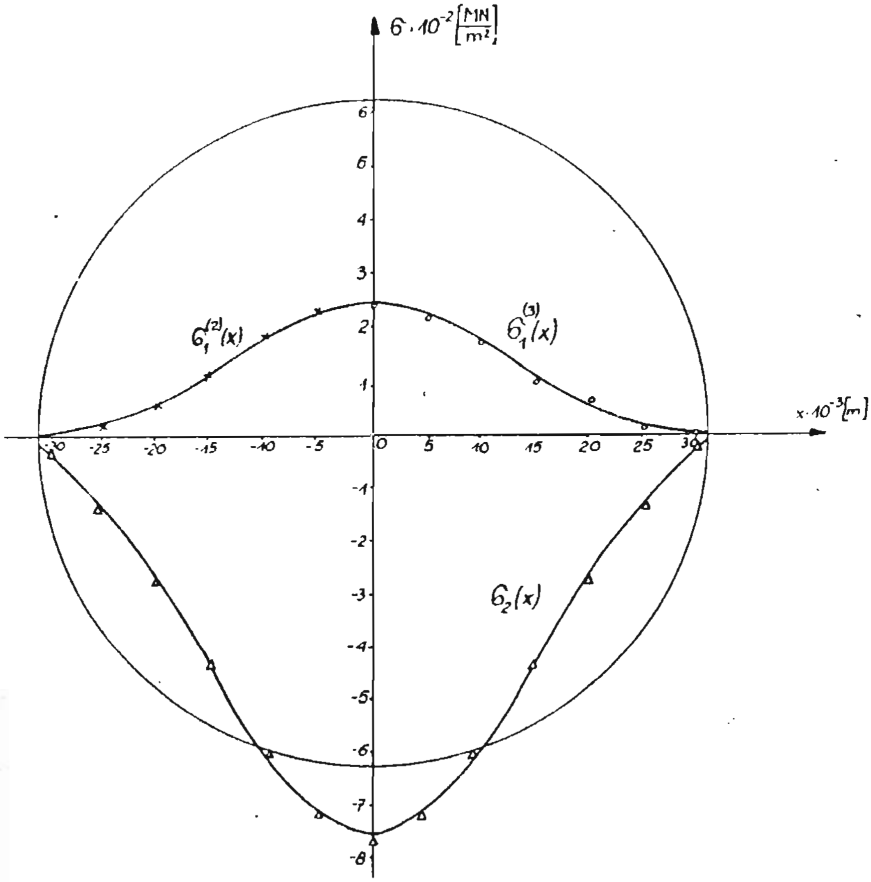


Fig. 10. Variation $\sigma_1^{(2)}$, $\sigma_1^{(3)}$ and $\sigma_2$ versus $x$ drawn on the basis of the data received from: Δ – light running through the model in the direction $x_1$, × – in the direction $x_2$, o – in the direction respectively $x_3$, — theoretical solution

Introducing $\Delta m_k = M_k$, $\Delta x_k = X_k$ we can calculate an absolute error of expressions

$$S_2 = C_\sigma \frac{\sigma_2}{\lambda} = \frac{M_1}{X_1}$$
$$S_1^{(2)} = C_\sigma \frac{\sigma_1^{(2)}}{\lambda} = \frac{1}{\sin^2 \Theta_2}\Big(\frac{M_2}{X_2} - \frac{M_1}{X_1}\cos^2\Theta_2\Big) \tag{7.7}$$
$$S_1^{(3)} = C_\sigma \frac{\sigma_1^{(3)}}{\lambda} = \frac{1}{\sin^2 \Theta_3}\Big(\frac{M_1}{X_1} - \frac{M_3}{X_3}\Big)$$

taking into account quantities $M_k$, $X_k$, $\Theta_k$ $(k = 1,2,3)$ and according to formulas

$$\delta S_2 = \frac{\partial S_2}{\partial M_1}\delta M_1 + \frac{\partial S_2}{\partial X_1}\delta X_1$$
$$\delta S_1^{(2)} = \frac{\partial S_1^{(2)}}{\partial M_1}\delta M_1 + \frac{\partial S_1^{(2)}}{\partial M_2}\delta M_2 + \frac{\partial S_1^{(2)}}{\partial X_1}\delta X_1 + \frac{\partial S_1^{(2)}}{\partial X_2}\delta X_2 + \frac{\partial S_1^{(2)}}{\partial \Theta_2}\delta\Theta_2$$
$$\delta S_1^{(3)} = \frac{\partial S_1^{(3)}}{\partial M_1}\delta M_1 + \frac{\partial S_1^{(3)}}{\partial M_3}\delta M_3 + \frac{\partial S_1^{(3)}}{\partial X_1}\delta X_1 + \frac{\partial S_1^{(3)}}{\partial X_3} + \frac{\partial S_1^{(3)}}{\partial \Theta_3}\delta\Theta_3 \tag{7.8}$$

where

$\delta M_1 = \delta M_2 = \delta M_3 = \delta M$ – accuracy of reading the parameter $m$ in the direction $x_k$,

$\delta X_1 = \delta X_2 = \delta X_3 = \delta x X$ – accuracy of coordinates $x_k$ reading,

$\delta\Theta_2 = \delta\Theta_3 = \delta\Theta$ – accuracy of locating the model towards the light source.

Calculating derivatives appearing in the formula we finally get

$$\delta S_2 = \frac{1}{X_1}\Big(\delta M - \frac{M_1}{X_1}\delta X\Big)$$
$$\delta S_1^{(2)} = \frac{1}{X_1X_2\sin^2\Theta_2}\Big[(X_1 - X_2\cos^2\Theta_2)\delta M + \frac{1}{X_1X_2}(M_1X_2^2\cos^2\Theta_2 -$$
$$-M_2X_1^2)\delta X + 2\frac{\cos\Theta_2}{\sin\Theta_2}(M_1X_2 - M_2X_1)\delta\Theta\Big] \tag{7.9}$$
$$\delta S_1^{(3)} = \frac{1}{X_1X_3\sin^2\Theta_3}\Big[(X_3 - X_1)\delta M - \frac{1}{X_1X_3}(M_1X_3^2 - M_3X_1^2)\delta X -$$
$$-2\frac{\cos\Theta_3}{\sin\Theta_3}(M_1X_3 - M_3X_1)\delta\Theta\Big].$$

Values of $\delta S_2$, $\delta S_1^{(2)}$, $\delta S_1^{(3)}$ were calculated, as an example, for a point of coordinates $x = 0$ [m] basing on quantities $M_k$, $k$, $\Theta_k$ read with the accuracy $\delta M = 0.1$ [order], $\delta X = 0.001$ [m] and $\delta\Theta = 1^\circ$. Calculated values are $\delta S_2 = 37\% S_2$, $\delta S_1^{(2} = 37\% S_1$, $\delta S_1^{(3)} = 14\% S_1$. Increase in measurement accuracy of the quantity

$m$ to the value $\delta M = 0.01$ [order] and increase of accuracy in redaing the coordinates $x_k$ to $\delta X = 0.0005$ [m], causes the decrease in percentage errors to the value $\delta S_2 = 12\% S_2$, $\delta S_1^{(2)} = 8\% S_1$, $\delta S_1^{(3)} = 6\% S_1$. Possibility of increasing accuracy of results can be achieved by reconstruction of the test stand: introducing additional movement of the model along the direction of the light course, supplying this movement with a micrometer screw and determining places $J_{p_k} = 0$, $J_{q_k} = 0$ by a phototensor, introducing reading of the value m on the scale of micrometer screw.

*Praca wpłynęła do Redakcji dnia 26 stycznia 1988 roku*